Developmental Cell, Vol. 2, 41–54, January, 2002, Copyright ©2002 by Cell Press

Central Spindle Assembly and Cytokinesis Require a Kinesin-like Protein/RhoGAP Complex with Microtubule Bundling Activity

Masanori Mishima, Susanne Kaitna, and Michael Glotzer[1]
Research Institute of Molecular Pathology
Dr. Bohr-Gasse 7
A-1030 Vienna
Austria

Summary

A late step in cytokinesis requires the central spindle, which forms during anaphase by the bundling of antiparallel nonkinetochore microtubules. Microtubule bundling and completion of cytokinesis require ZEN-4/CeMKLP-1, a kinesin-like protein, and CYK-4, which contains a RhoGAP domain. We show that CYK-4 and ZEN-4 exist in a complex in vivo that can be reconstituted in vitro. The N terminus of CYK-4 binds the central region of ZEN-4, including the neck linker. Genetic suppression data prove the functional significance of this interaction. An analogous complex, containing equimolar amounts of a CYK-4 ortholog and MKLP-1, was purified from mammalian cells. Biochemical studies indicate that this complex, named centralspindlin, is a heterotetramer. Centralspindlin, but not its individual components, strongly promotes microtubule bundling in vitro.

Introduction

A critical step in the cell division cycle is the formation of two separate daughter cells by cytokinesis. The actomyosin-containing contractile ring pulls the overlying plasma membrane toward the center of the cell where it reaches a microtubule-based structure called the central spindle. The central spindle is essential for completion of cytokinesis in animal cells (for a review, see Straight and Field, 2000). Central spindle assembly begins in early anaphase when nonkinetochore spindle microtubules become bundled. The microtubule bundles that make up the central spindle span the interpolar region of the anaphase spindle. There is a narrow region of overlap between the two sets of antiparallel microtubules (Mastronarde et al., 1993). These bundles become compacted during cytokinesis and eventually develop into the cell midbody.

In many animal cells, including the early *C. elegans* embryo, the central spindle plays a crucial role during the late stages of cytokinesis. This was first established by studies of embryos deficient in the kinesin-like protein ZEN-4/CeMKLP-1 (hereafter referred to as ZEN-4; Powers et al., 1998; Raich et al., 1998). ZEN-4-depleted embryos fail to assemble the central spindle but initiate cytokinesis normally, and the cleavage furrow ingresses to near completion but subsequently regresses. ZEN-4 may play a direct role in central spindle assembly since, in wild-type embryos, it is highly concentrated in a narrow region of the spindle midzone; this region may correspond to the region of microtubule overlap.

There is strong evidence that the function of ZEN-4 is conserved widely among metazoans. The mammalian ortholog of ZEN-4, MKLP-1/CHO1 (hereafter referred to as MKLP-1), was the founding member of this subfamily of kinesins. Although initial antibody microinjection experiments implicated MKLP-1 in mitotic progression (Nislow et al., 1992), recent genetic evidence indicates that MKLP-1 family members function specifically in cytokinesis. As mentioned above, the nematode ortholog is essential for cytokinesis, as is the *Drosophila* ortholog, *pavarotti* (Adams et al., 1998). MKLP-1 was shown to have plus end-directed microtubule motility in vitro (Nislow et al., 1992). Overexpression of MKLP-1 in cultured cells induces antiparallel microtubule bundles (Sharp et al., 1996). Though ZEN-4 may have the capacity to promote microtubule bundling upon overexpression, during cytokinesis it cannot be sufficient since, in vivo, there are additional factors beside ZEN-4 that are essential for central spindle assembly.

The kinesin superfamily is quite diverse, containing three major classes based upon the position of the catalytic core. The largest class, the KIN-N class, of which ZEN-4 is a member, has N-terminal motor domains (see Vale and Fletterick, 1997; Vale and Milligan, 2000 for reviews). Members of this class have been implicated in a variety of biological processes including chromosome movement, centrosome separation, vesicle trafficking, and establishment of organismal polarity. These microtubule motors are believed to carry out these diverse functions by association with accessory proteins that enable them to attach specifically to chromosomes, centrosomes, vesicles, etc. Although many kinesins have been described, far fewer accessory proteins have been characterized. Thus the biological function of most kinesins is not yet fully understood at the molecular level. On the other hand, the mechanism of microtubule-based motility of conventional kinesin, a KIN-N that is the founding member of the entire superfamily of kinesins, and of NCD, a motor with a C-terminally positioned catalytic domain (KIN-C), have been studied at atomic resolution. The conformational changes that convert chemical energy into mechanical force are known and the critical regions of the catalytic core have been identified (Kikkawa et al., 2001; Kull et al., 1996; Rice et al., 1999; Sablin et al., 1996). This basic mechanism of force generation is undoubtedly utilized by most, if not all, kinesin superfamily members. It is therefore important to understand in more detail how various kinesin family members mediate individual processes within the cell and to relate these findings to the mechanism of force production.

Recently, we have identified a Rho family GAP protein, CYK-4, that appears to have a functional connection to the ZEN-4 kinesin-like protein (Jantsch-Plunger et al., 2000). The phenotype of *cyk-4* mutant embryos is indistinguishable from that of embryos lacking ZEN-4; in particular, interpolar microtubules do not become bundled to form the central spindle. CYK-4 and ZEN-4 colocalize

[1]Correspondence: mglotzer@nt.imp.univie.ac.at

on the central spindle and they are interdependent for their localization. Finally, we found a synthetic lethal interaction between temperature-sensitive alleles of *cyk-4* and *zen-4*. Taken together, these data raise the possibility that CYK-4 and ZEN-4 interact in vivo and that this interaction is essential for central spindle assembly and for cytokinesis. Here we show that CYK-4 and ZEN-4 associate in vivo. These proteins also efficiently associate in vitro, and we have used an in vitro binding assay to dissect the regions of both proteins that are necessary and sufficient for this interaction. We show that the protein encoded by the temperature-sensitive allele *cyk-4(t1689)* is defective in binding to ZEN-4. We have found mutations in the CYK-4 binding region of *zen-4* that suppress *cyk-4(t1689)*, providing strong evidence for the importance of the interaction for progression of cytokinesis. The human orthologs of CYK-4 and ZEN-4, HsCYK-4/MgcRacGAP and MKLP-1, are also in a complex which we have purified. This complex contains equimolar amounts of HsCYK-4 and MKLP-1. Both of these proteins localize to the central spindle and to division remnants, as do the nematode orthologs. In vitro, CYK-4 and ZEN-4 together, but not individually, promote the formation of large bundles of microtubules. Thus we have identified an evolutionarily conserved protein complex that is essential for central spindle assembly.

Results

CYK-4 and ZEN-4 Form a Complex In Vivo and In Vitro

To test whether CYK-4 and ZEN-4 exist in a stable biochemical complex, we performed immunoprecipitation experiments using extracts prepared from early *C. elegans* embryos. When embryo extracts were immunoprecipitated using anti-CYK-4 antibodies, a significant amount of ZEN-4 coimmunoprecipitated suggesting the existence, in vivo, of a stable complex containing CYK-4 and ZEN-4 (Figure 1A).

To determine whether CYK-4 and ZEN-4 are competent to interact in the absence of other nematode proteins, the two proteins were produced by in vitro translation and subjected to immunoprecipitation. When CYK-4 and ZEN-4 (fused to the chitin binding domain; CBD) were translated in vitro and subsequently mixed, both proteins could be recovered in high yield by chitin beads (Figure 1B). The coprecipitation of CYK-4 was dependent on ZEN-4; CYK-4 was not recovered on chitin beads when ZEN-4 was substituted by CBD alone. Moreover, when luciferase was substituted for CYK-4, it did not coprecipitate with ZEN-4. The association between CYK-4 and ZEN-4 could also be detected when anti-CYK-4 antibodies were used to retrieve the complex (Figure 1C).

Delineation of the Region of CYK-4 Necessary to Bind to ZEN-4

Since the binding between CYK-4 and ZEN-4 could be easily reconstituted using in vitro-translated proteins, we used this assay to dissect the regions of the two proteins that mediate this interaction. We first concentrated on CYK-4. The N-terminal 34 amino acids of

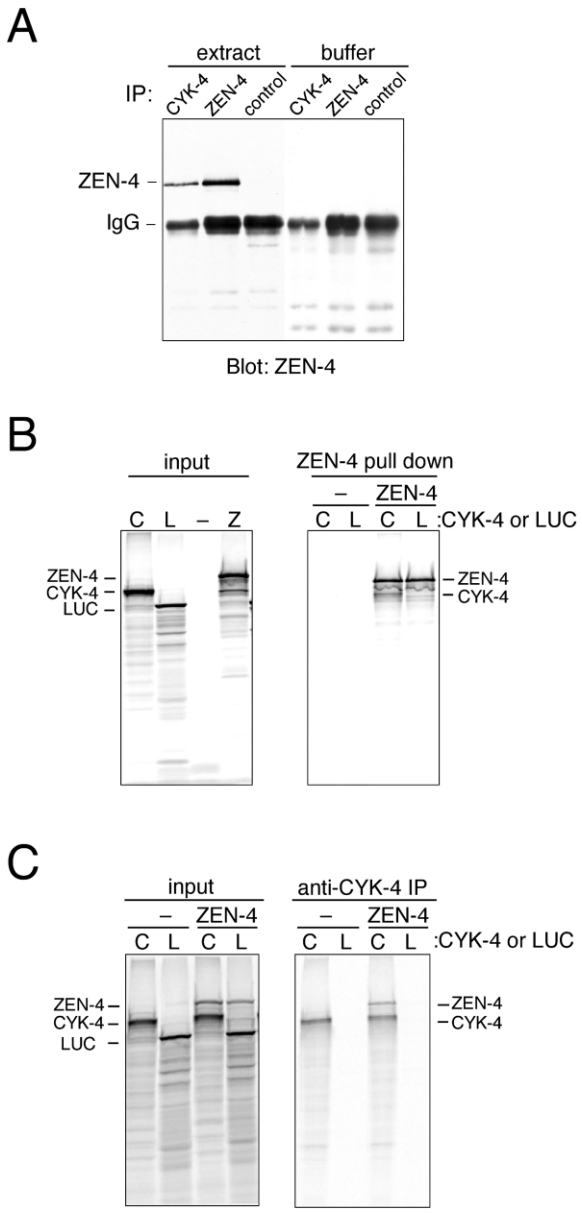

Figure 1. CYK-4 and ZEN-4 Associate In Vivo and In Vitro

(A) Immunoprecipitation was performed on worm embryo extracts with antibodies directed against CYK-4, ZEN-4, or nonspecific rabbit IgG. The immunoprecipitates were resolved on SDS-PAGE gels followed by Western blotting with an anti-ZEN-4 antibody. Mock immunoprecipitation without extract was included to control for crossreactivity with the antibodies. ZEN-4 specifically coimmunoprecipitated with CYK-4.

(B) ^{35}S-labeled CYK-4 (or luciferase; LUC) and chitin binding domain (CBD)-tagged ZEN-4 (or CBD alone) were separately expressed by in vitro translation (left panel). Translation reactions were mixed and incubated in the indicated combinations and CBD-ZEN-4 or CBD alone were recovered with chitin beads (right panel). In this and all other gels in this paper, the input lanes contain the same amount of translation product as was added to the beads used for precipitation. The precipitates were resolved on SDS-PAGE gels and the labeled products were detected by a phosphoimager. CYK-4 copurified with CBD-ZEN-4 while the luciferase control did not.

(C) CYK-4 (or luciferase) and CBD-ZEN-4 (or CBD alone) were coexpressed as ^{35}S-labeled proteins in the indicated combinations (left panel). CYK-4 was immunoprecipitated with an anti-CYK-4 antibody (right panel). ZEN-4 coimmunoprecipitated with CYK-4.

CYK-4 are poorly conserved and are followed by an ~90 amino acid region predicted to form a coiled coil (see schematic in Figure 2E). The C-terminal 250 amino acids contain a RhoGAP domain that is active in vitro against RhoA, Rac1, and Cdc42 (Jantsch-Plunger et al., 2000). The RhoGAP domain is preceded by a C1 domain, a cysteine-rich domain that may mediate interactions with diacylglycerol (Hurley and Meyer, 2001). Truncations of the C terminus of CYK-4 revealed that the ZEN-4 binding region is contained within the N-terminal 232 amino acids (fragment c5; Figure 2A). Further truncations within this region indicated that residues 1–120 (fragment c8; from the N terminus to the end of the coiled-coil region) are sufficient to bind efficiently to ZEN-4 (Figure 2B). Further deletions within this minimal domain impaired binding. Neither a near full-length version of CYK-4 lacking only the N-terminal 34 amino acids (fragment c1) nor a derivative lacking the coiled-coil domain (fragment c3) was able to bind ZEN-4 (Figure 2A). Thus the ability of CYK-4 to interact with ZEN-4 depends on the N-terminal 120 residues of CYK-4 (Figure 2E).

Delineation of the ZEN-4 Region Required to Bind CYK-4

We next used the in vitro assay to define the region of ZEN-4 that binds to the N terminus of CYK-4. Initially, we compared the CYK-4 binding activity of full-length ZEN-4 (z0) to that of three C-terminal deletion fragments of ZEN-4: a C-terminal truncation derivative that lacks the domain following the coiled-coil domain (z1), the catalytic core domain and the linker region (z2), and the N-terminal catalytic core alone (z3). The full-length protein (z0) bound CYK-4 with high affinity, as did the next longer fragment (z1), but the two smaller fragments did not interact with CYK-4 (Figure 2C). Next, we examined whether the binding activity could be further localized within the central region of ZEN-4. A minimal binding domain (z7) consisting of 169 amino acids was defined. This region appears to consist of two elements, the linker region and the coiled coil; neither of these individual elements had detectable binding activity on their own (Figure 2D). These data are summarized in Figure 2E.

The interaction of CYK-4 with the neck linker/coiled-coil region of ZEN-4 is particularly interesting in light of recent studies that indicate that in conventional kinesin, the neck linker region is critical for force production by this mechanochemical enzyme (Case et al., 2000; Rice et al., 1999; see Discussion).

The Product of *cyk-4(t1689ts)* Does Not Interact with ZEN-4

Although the amino-terminal region of CYK-4 exhibits poor sequence conservation at the primary sequence level (Figure 7A), our earlier studies indicated that this region is crucial for its in vivo function since the *cyk-4(t1689)* allele contains a substitution mutation at position 15. Since this point mutation maps into the ZEN-4 binding region (Figure 2E) and since, in vivo, this mutation affects the ability of CYK-4 and ZEN-4 to colocalize, we tested whether this mutation also affects the ability of these two proteins to interact in vitro. This substitution, S15L, was engineered into the CYK-4 expression construct (c4) and used for ZEN-4 binding assays. Whereas an interaction between CYK-4 and ZEN-4 can be readily detected, the S15L mutant does not interact with ZEN-4 (Figure 2A). This experiment indicates that the destabilization of the interaction between CYK-4 and ZEN-4 may be the primary defect in *cyk-4(t1689ts)* embryos.

In Vivo Evidence for the CYK-4/ZEN-4 Interaction

To gain further insight into the mechanism of CYK-4 function in vivo, we sought to identify suppressors of the *cyk-4(t1689ts)* mutation. Homozygous *cyk-4(t1689ts)* animals were mutagenized and allowed to self-fertilize for two generations at the permissive temperature. When the F2 animals reached early adulthood, the temperature was shifted to 20°C to impose a selection for fertile animals carrying presumptive suppressor mutations. We identified 18 suppressor mutations (see Experimental Procedures). Intragenic suppressors were identified by sequencing of the *cyk-4* locus, PCR amplified from the suppressor strains. Six suppressor strains contained an additional point mutation in the N terminus of CYK-4; all of the mutations coded for amino acid substitutions within the biochemically defined ZEN-4 binding region (Figure 3A).

In addition to the mutations found within the *cyk-4* gene itself, we also identified extragenic suppressor mutations. One suppressor strain that did not contain mutations within the *cyk-4* gene was characterized in detail. The suppressor activity was mapped to the central region of chromosome IV using single-nucleotide polymorphisms. Since the *zen-4* gene maps to this region, the coding region of the *zen-4* gene was sequenced. This strain, *xs82*, was found to contain a point mutation that causes a substitution of glutamic acid for a lysine at position 502 (Figure 3A). Importantly, this substitution maps within the region of ZEN-4 that mediates the interaction with CYK-4 in vitro. This substitution allele, E502K, does not cause a detectable phenotype on its own. Sequencing of the ZEN-4 locus in the other suppressor strains revealed that seven other strains contained point mutations in ZEN-4, six of which are localized within the biochemically defined CYK-4 binding domain (Figure 3A).

As mentioned above, CYK-4(S15L) is unable to interact with ZEN-4 in the in vitro binding assay. If the immediate consequence of the S15L substitution in the N terminus of CYK-4 is a defect in ZEN-4 binding, then an extragenic suppressor mutation in *zen-4* that rescues *cyk-4(t1689)* might restore binding to CYK-4(S15L). To test this possibility, we translated either the wild-type CYK-4 fragment (c5) or a mutated version encoding the S15L substitution and mixed this product with a fragment of ZEN-4 (z4) carrying either the wild-type glutamic acid at position 502 or the lysine substitution allele. Wild-type CYK-4 fragment bound equally well to wild-type and the E502K derivative of ZEN-4. As discussed above, CYK-4(S15L) is unable to bind to wild-type ZEN-4. However, CYK-4(S15L) was able to bind to ZEN-4(E502K), though this interaction was weaker than that seen with the wild-type proteins (Figure 3B). These data, together with the genetic suppression, prove that the interaction between the N terminus of CYK-4 and the central region of ZEN-4 is crucial for their function in vivo.

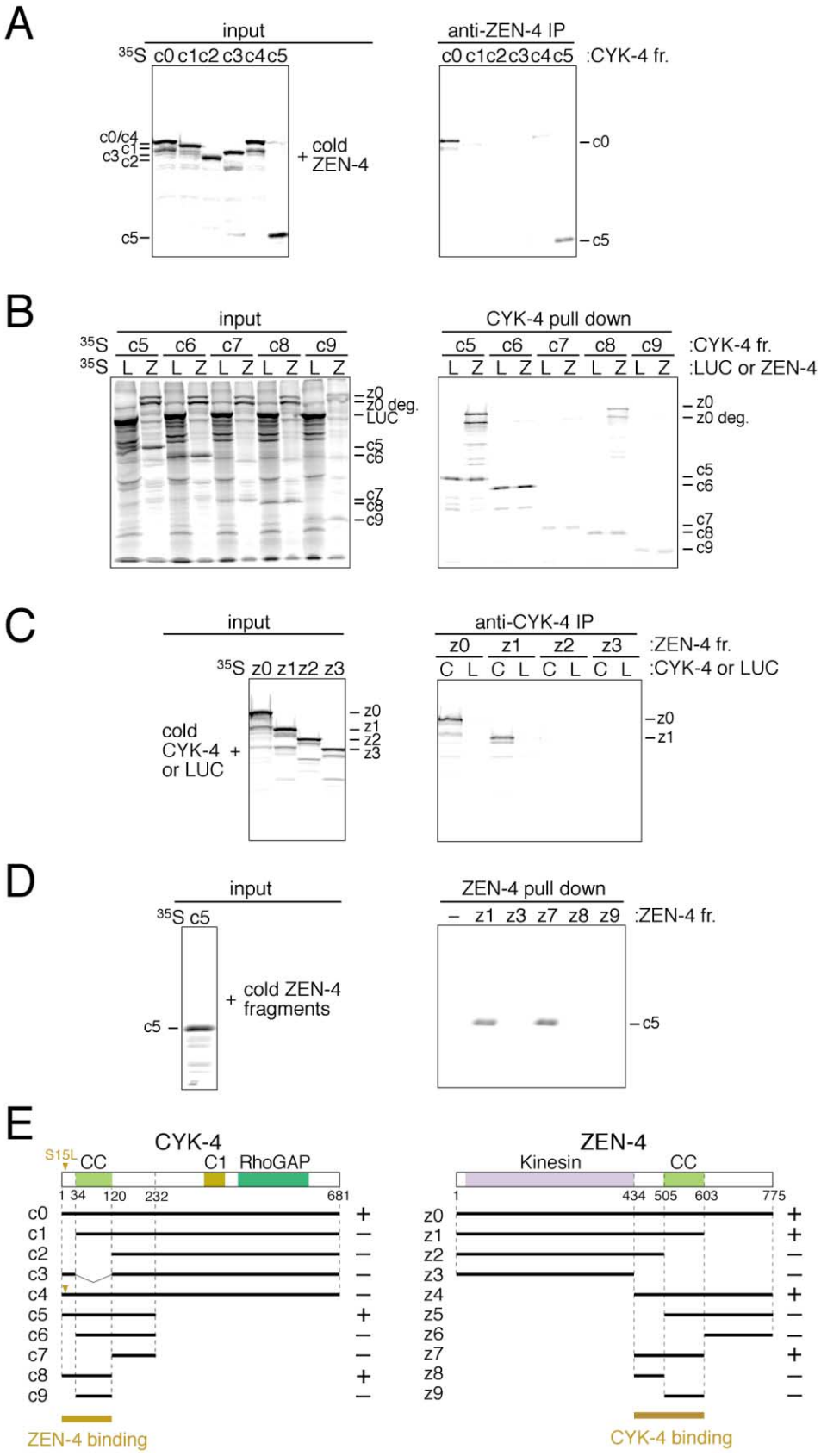

Figure 2. The N Terminus of CYK-4 Is Necessary and Sufficient to Bind to the Central Region of ZEN-4

The interacting regions of CYK-4 and ZEN-4 were defined using an in vitro binding assay.

(A) CYK-4 derivatives c0, c1, c2, c3, c4, and c5 (see [E]) were expressed as ^{35}S-labeled proteins by in vitro translation (left panel). The reaction

In Vivo, the Majority of ZEN-4 Is in a Complex with CYK-4

To gain insight into the molecular architecture of the CYK-4/ZEN-4 complex and to determine whether the majority of ZEN-4 is in a complex with CYK-4 in vivo, we performed sucrose density gradient centrifugation experiments with extracts prepared from *C. elegans* embryos. When wild-type extracts are prepared in the presence of 0.6 M NaCl, ZEN-4 migrates as a symmetrical 9 S peak (Figure 3C). CYK-4 migrates at an identical S value (data not shown). To determine whether the migration of ZEN-4 on sucrose gradients was dependent on its association with CYK-4, we took advantage of the finding that the *cyk-4(t1689)* allele is specifically defective in its ability to bind to ZEN-4. When extracts were prepared from *cyk-4* mutant embryos and subjected to sucrose density centrifugation, ZEN-4 migrates as a symmetrical peak with a sedimentation value of 6 S, significantly less dense than ZEN-4 sediments in wild-type extracts (Figure 3C). These data indicate that, in vivo, the majority of ZEN-4 is in a complex with CYK-4.

CYK-4 and ZEN-4 Self-Associate

Thus far, we have established that central spindle assembly is dependent on an interaction between CYK-4 and ZEN-4 and have defined the regions of both proteins that are required for this interaction. Interestingly, both binding domains contain coiled-coil regions. Since coiled coils can be dimerization motifs and since many kinesin motors are often composed of two motor domains tethered by a coiled coil, we examined whether CYK-4 and ZEN-4 are able to self-associate.

To assess whether CYK-4 self-associates, we coexpressed full-length CYK-4 and the CYK-4 fragment (c5). As a control, the full-length protein was substituted by the truncated version lacking the N-terminal 120 amino acids (and hence the coiled-coil domain; c2). The longer CYK-4 fragments were immunoprecipitated with an antibody directed against the C-terminal region of CYK-4, and the coimmunoprecipitation of the short N-terminal fragment was assessed. The N-terminal fragment (c5) bound to full-length CYK-4 (c0) but not to CYK-4 lacking the N-terminal domain (c2; Figure 4A). These data demonstrate that CYK-4 self-associates. This association is likely mediated by the coiled-coil domain.

The capacity of ZEN-4 to self-associate was examined using a similar strategy. Full-length ZEN-4 was coexpressed with affinity-tagged deletion derivatives of ZEN-4. Neither the N-terminal region (z2) nor the C-terminal region (z6) of ZEN-4 bound appreciably to full-length ZEN-4, but two fragments of ZEN-4 (z5 and z7) bound to full-length ZEN-4 (Figure 4B). The region common to these two fragments consists of residues 505–603, which is the region predicted to form a coiled coil.

The ability of CYK-4 and ZEN-4 to self-associate in vitro raises the possibility that in vivo, the CYK-4/ZEN-4 complex may contain, at a minimum, two molecules each of CYK-4 and ZEN-4.

The Human Orthologs of CYK-4 and ZEN-4, HsCYK-4 and MKLP-1, Interact In Vivo and Colocalize

In *C. elegans*, CYK-4 and ZEN-4 associate in vivo and in vitro, and this complex is important for central spindle assembly and cytokinesis. To extend these findings, we evaluated whether mammalian cells contained a stable complex containing the human orthologs of these proteins, HsCYK-4/MgcRacGAP (Hirose et al., 2001; Toure et al., 1998; Wooltorton et al., 1999) and MKLP-1, respectively. Extracts were prepared from mitotic HeLa cells, and antibodies directed against HsCYK-4 or MKLP-1 were used for immunoprecipitation followed by Western blotting. MKLP-1 could be coimmunoprecipitated with anti-HsCYK-4 antibodies and vice versa (Figure 5A). The immunoblots revealed that small amounts of HsCYK-4 and MKLP-1 migrate with reduced mobility, likely due to phosphorylation.

To obtain evidence that these proteins play a similar role in human cells as was shown previously for the nematode proteins, we examined the localization of HsCYK-4 and MKLP-1 in cultured (HeLa) human cells. During all stages of the cell cycle, the two proteins precisely colocalize (Figure 5B, panels a′–d′). In early anaphase, the two proteins localize to the nascent central spindle (panels a and a′). During mid-to-late anaphase they localize to short segments in the central spindle (panels b and b′). Three-dimensional reconstruction of optically sectioned anaphase cells revealed that each bundle of microtubules in the central spindle is labeled at its distal end by MKLP-1 antibodies (see Supplemental Movie S1 at http://www.developmentalcell.com/cgi/content/full/2/1/41/DC1). The MKLP-1 staining region is

products were incubated with unlabeled full-length ZEN-4 and, after incubation, ZEN-4 was immunoprecipitated with an anti-ZEN-4 antibody (right panel). Two fragments of CYK-4, c0 and c5, coimmunoprecipitated with ZEN-4. Full-length CYK-4 bearing the point mutation of S15L (c4) only weakly associates with ZEN-4.

(B) CBD-CYK-4 fragments (c5, c6, c7, c8, and c9) and full-length ZEN-4 (or luciferase as a control) were coexpressed as ^{35}S-labeled proteins by in vitro translation (left panel). CBD-CYK-4 fragments were affinity purified (right panel). ZEN-4 copurified with CYK-4 fragments c5 and c8, but not with fragments c6, c7, or c9.

(C) Full-length ZEN-4 (z0) and C-terminal deletion fragments of ZEN-4 (z1, z2, and z3) were ^{35}S-labeled by in vitro translation and incubated with unlabeled CYK-4 (or luciferase as a control; left panel). CYK-4 was precipitated with anti-CYK-4 antibody (right panel). Full-length ZEN-4 and the z1 deletion derivative coprecipitated with CYK-4, while shorter fragments (z2 and z3) did not.

(D) CBD-tagged fragments of ZEN-4 (z1, z3, z7, z8, and z9) were expressed in an unlabeled form and incubated with ^{35}S-labeled CYK-4 (c5; left panel). ZEN-4 fragments were pulled down by affinity chromatography using chitin beads (right panel). CYK-4 (c5) copurified with ZEN-4 deletion derivatives z1 and z7, but not with z3, z8, and z9.

(E) A summary of the CYK-4 and ZEN-4 derivatives tested. Binding activity is denoted (+ or −). The minimal derivative that retains ZEN-4 binding activity is c8, which corresponds to residues 1–120 of CYK-4. This region contains a coiled-coil (CC) region and an N-terminal extension. The minimal derivative that retains CYK-4 binding activity is z7, which corresponds to residues 435–603 of ZEN-4. This region contains a "neck" region C-terminal to the kinesin catalytic core and a coiled-coil region.

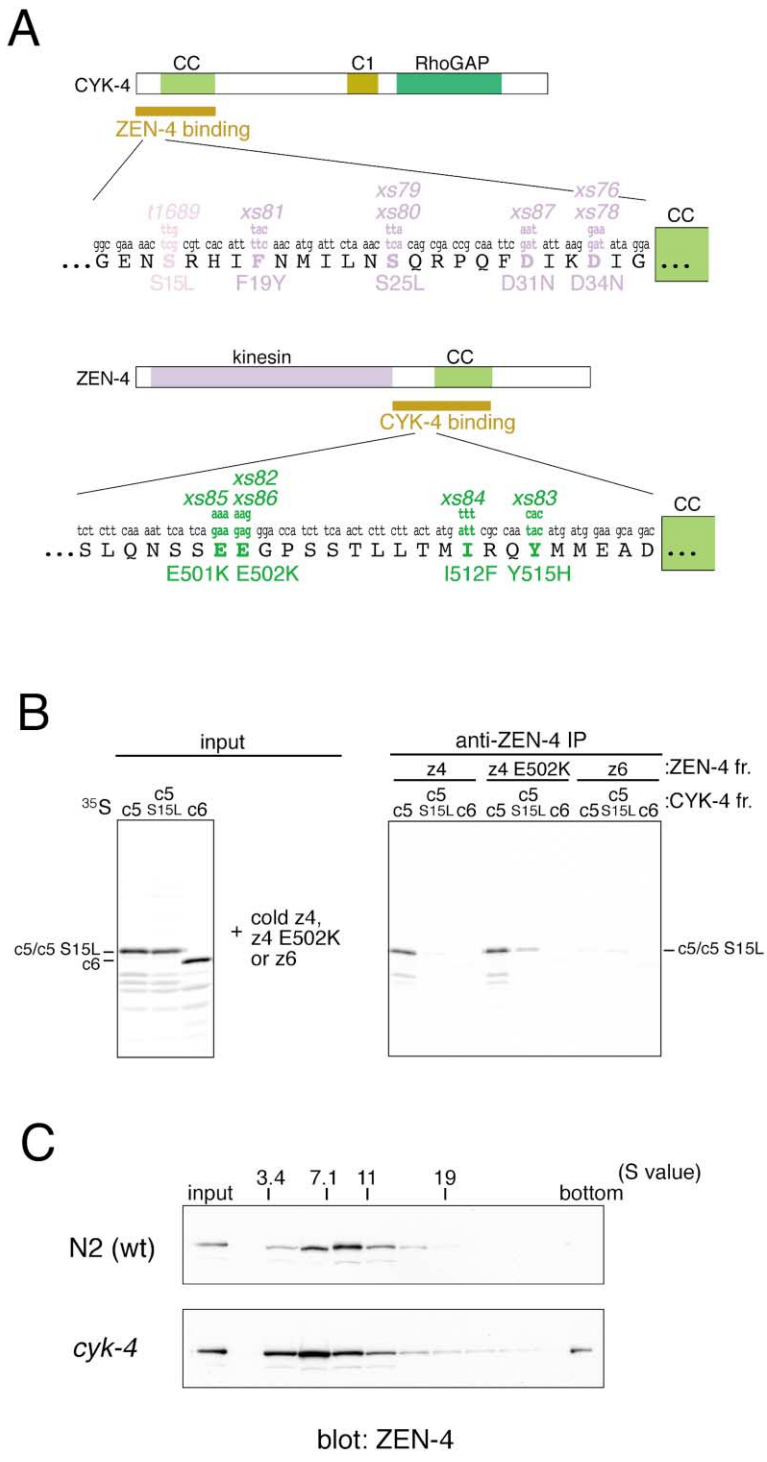

Figure 3. A Complex of CYK-4 and ZEN-4 Is Required for Function In Vivo

(A) Several point mutations in the *cyk-4* and *zen-4* coding region were isolated as suppressors of *cyk-4(t1689ts)*. The nature of 11 alleles are shown in the figure; two additional substitution mutations in ZEN-4 were isolated, E340K and G454E. *zen-4(xs82)*, which causes an E502K substitution, was studied in detail.

(B) ZEN-4(E502K) binds to CYK-4(S15L). CYK-4 fragments c5 and c5(S15L) were expressed as ^{35}S-labeled proteins and incubated with unlabeled ZEN-4 fragments (z4, z4(E502K), and z6). ZEN-4 fragments were precipitated with anti-ZEN-4 antibody. CYK-4 fragment c5 coprecipitated with ZEN-4 (z4) but not with ZEN-4 (z6). The S15L mutation in CYK-4 fragment c5 abolishes its ability to bind to ZEN-4 (z4). However, the suppressor mutation in ZEN-4 partially recovered this interaction [CYK-4 c5(S15L) and ZEN-4 z4(E502K)]. The ZEN-4(E502K) substitution does not affect binding to wild-type CYK-4.

(C) The majority of ZEN-4 is in a complex with CYK-4 in vivo. Extracts were made from wild-type (N2) embryos or *cyk-4(t1689ts)* embryos. Sedimentation of ZEN-4 was analyzed by sucrose density gradient centrifugation followed by Western blotting. The samples were spiked with the indicated standards, which ran identically in the two gradients. ZEN-4 from wild-type embryos sediments at 9 S, whereas ZEN-4 from *cyk-4* mutant embryos sediments at 6 S.

0.93 ± 0.25 μm in length (n = 56); this region largely corresponds to the region that appears deficient in tubulin staining, but this is a known artifact caused by epitope masking (Saxton and McIntosh, 1987). The extent of staining is somewhat narrower than previous ultrastructural determinations of the extent of microtubule overlap (>2 μm; Mastronarde et al., 1993). Later in cleavage, both proteins localize to a discrete, central portion of the midbody (panels c and c′). These observations are consistent with previous studies of the individual subunits (Hirose et al., 2001; Sellitto and Kuriyama, 1988). During interphase, some cells contain HsCYK-4 and MKLP-1 in the nucleus, whereas others do not. This is likely due to cell cycle-regulated accumulation of these factors since, upon G2 arrest, HsCYK-4 and MKLP-1 accumulate in the nucleus of all cells (data not

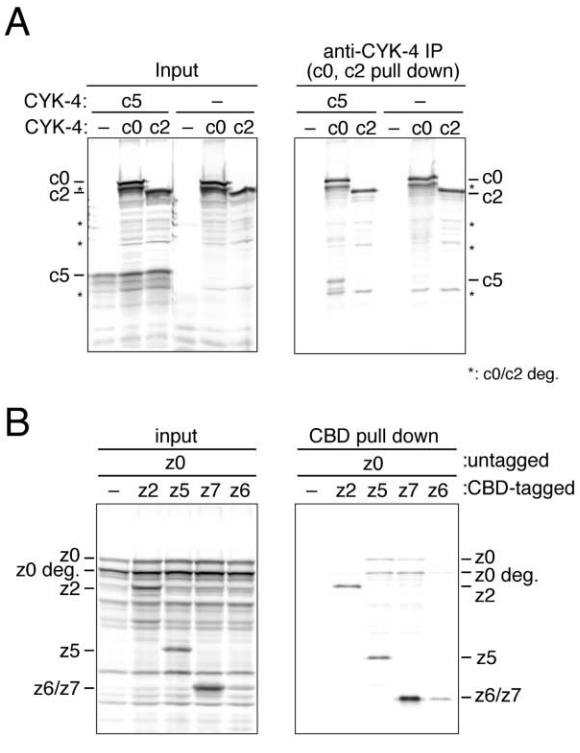

Figure 4. CYK-4 and ZEN-4 Self-Associate through Their Coiled-Coil Domains

CYK-4 and ZEN-4 are both able to self-associate.

(A) CYK-4 fragment (c5) (residues 1–232) was coexpressed as a ^{35}S-labeled protein with CYK-4 (c0) or (c2) (left panel). The CYK-4 fragments (c0) and (c2) were immunoprecipitated; fragment c5 is not recognized by this C-terminal antibody. CYK-4 fragment c5 coimmunoprecipitates with CYK-4 (c0), but not with CYK-4 (c2).

(B) CBD-tagged fragments of ZEN-4 (z2, z5, z7, or z6) were coexpressed with untagged ZEN-4 (z0) (left panel). CBD-tagged fragments were purified by affinity chromatography with chitin beads (right panel). Untagged ZEN-4 (z0) copurified with CBD-ZEN-4 (z5) and (z7), but not with ZEN-4 (z2) or (z6). The low extent of labeling of (z6) as compared to (z7) is attributable to low cysteine and methionine content of the C-terminal fragment.

shown). In addition, most cells contain brightly staining cortical spot or ring-like structures. These structures likely correspond to division remnants (panels d and d′); previous time-lapse microscopy with GFP-tagged CYK-4 and ZEN-4 in nematode embryos revealed that the central spindle matures into the midbody that later develops into a persistent spot or ring in the cell cortex. Thus there is a striking concordance between the biochemical properties and the subcellular localization of CYK-4/ZEN-4 in *C. elegans* embryos and HsCYK-4/MKLP-1 in human cells. Since the names of the individual proteins vary from species to species, we propose to call this complex "centralspindlin." To establish that centralspindlin performs a similar function in these two systems, HeLa cells were depleted of HsCYK-4 using RNAi. Cells depleted of HsCYK-4 did not assemble a well-organized central spindle and they failed to complete cell division (Figure 5C); 48% ($n = 151$) of cells treated with CYK-4 siRNA became polyploid or multinucleate in 72 hr compared to 2% ($n = 273$) in the mock-treated control. These data indicate that the function of centralspindlin is conserved from nematodes to humans.

To gain insight into the architecture of centralspindlin, we investigated the hydrodynamic properties of its constituents. Lysates were prepared from mitotic HeLa cells and run on sucrose density gradients. Western blotting of the gradient fractions indicated that HsCYK-4 and MKLP-1 comigrate on the gradients with an S value of 8 (Figure 5D). This sedimentation behavior is similar to that of centralspindlin extracted from *C. elegans* embryos. The two proteins also comigrated on a gel filtration column with an apparent molecular weight of 800 kDa (data not shown). Gel filtration chromatography cannot accurately estimate the native molecular mass of asymmetric particles. However, gel filtration data, combined with S value measurements, allow a more accurate estimation of the native molecular mass. When the experimental values of centralspindlin are combined in this way, the complex is estimated to have a native molecular weight of ~300 kDa.

To determine whether equimolar amounts of HsCYK-4 and MKLP-1 are present in centralspindlin and whether or not other proteins are also in the complex, we immunopurified the complex from the microtubule binding fraction prepared from mitotic cells. Antibodies specific for HsCYK-4 and MKLP-1 were used in parallel for the immunoprecipitation. Coomassie blue staining of both immunoprecipitates revealed two major bands (75 and 110 kDa) and one minor band (116 kDa; Figure 5E). Mass spectrometry analysis revealed that the 110 and 116 kDa bands are MKLP-1 and the 75 kDa band is HsCYK-4. No additional bands reproducibly coprecipitated with HsCYK-4 or MKLP-1. Given that (1) centralspindlin has a native molecular mass of ~300 kDa, (2) it does not appear to contain any proteins in addition to HsCYK-4 and MKLP-1, and (3) both components are capable of self-association, we conclude that centralspindlin is a tetramer containing two molecules each of HsCYK-4 and MKLP-1.

Centralspindlin Is Sufficient to Induce Microtubule Bundling In Vitro

To investigate whether centralspindlin is sufficient to induce microtubule bundling, CYK-4 and ZEN-4 were produced in insect cells using a baculovirus expression system. CYK-4 and ZEN-4 were individually purified to near homogeneity and the CYK-4/ZEN-4 complex was purified after coinfection with the two viruses (Figure 6A). A reconstituted complex, containing CYK-4/ZEN-4(z1), sediments in sucrose gradients with a similar S value as did the centralspindlin complex isolated from wild-type *C. elegans* embryos, and ZEN-4(z1) alone sediments with a similar pattern as did ZEN-4 in *cyk-4* mutant embryo extracts (data not shown). CYK-4 and ZEN-4 were then incubated individually or in combination with microtubules in the presence of the nucleotide analog AMP-PNP to stabilize the interaction between the motor protein and microtubules. The reactions were fixed, loaded onto a glycerol cushion, and sedimented onto a glass coverslip. The samples were labeled with antibodies specific for tubulin and CYK-4 or ZEN-4. In the samples that contained CYK-4 or ZEN-4 alone, little microtubule bundling was observed. When present simultaneously, CYK-4 and ZEN-4 induced extensive microtubule bundling (Figure 6B). Immunolocalization of

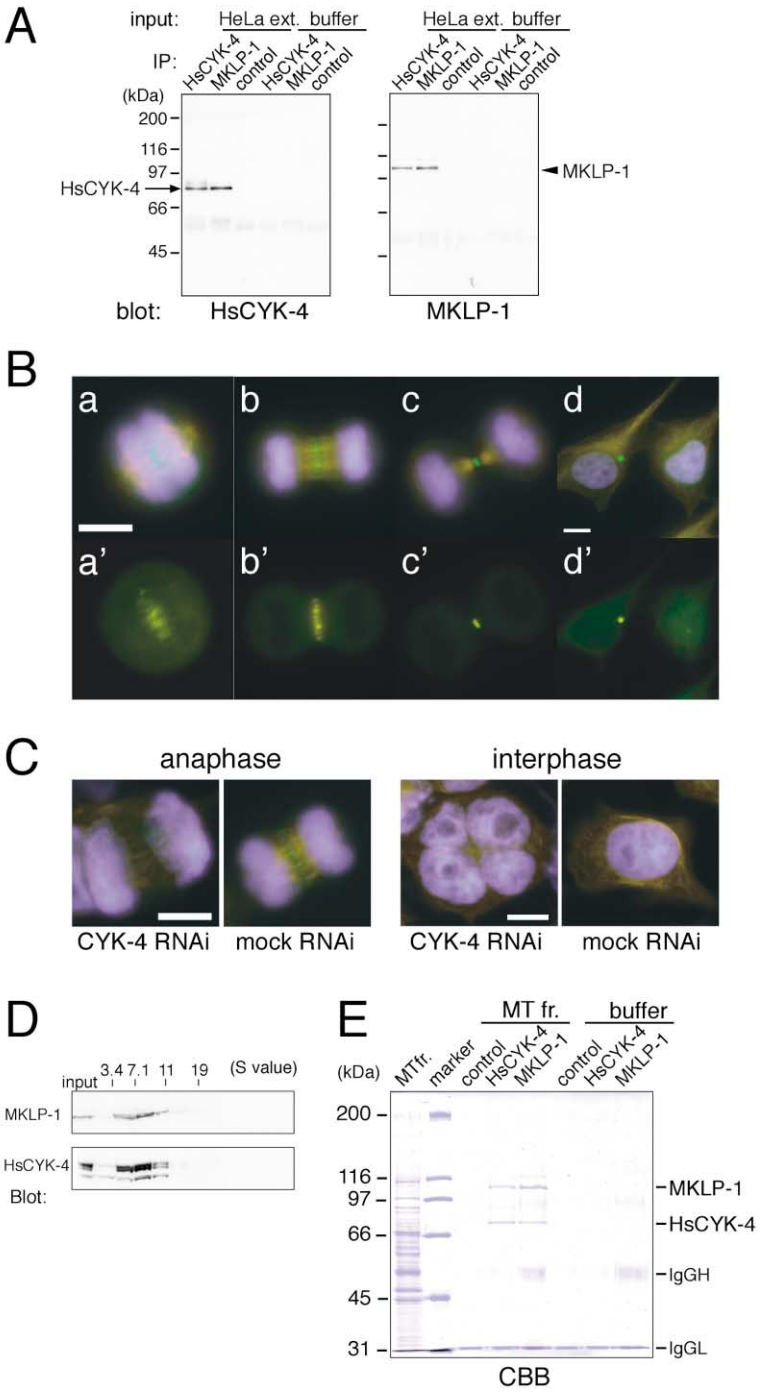

Figure 5. A Complex of MKLP-1 and HsCYK-4 in HeLa Cells

HsCYK-4/MgcRacGAP and MKLP-1, the human orthologs of CYK-4 and ZEN-4, respectively, exist as a complex in mitotic HeLa cells.

(A) HsCYK-4 and MKLP-1 were immunoprecipitated from HeLa cell lysate with specific rabbit antibodies and blotted with specific mouse antibodies. HsCYK-4 coimmunoprecipitated with MKLP-1 and vice versa.

(B) HsCYK-4 and MKLP-1 colocalize to the central spindle and the midbody. HeLa cells were fixed and immunostained with anti-CYK-4, anti-MKLP-1, and anti-tubulin antibodies, and DNA was stained with Hoechst. Shown are cells in early anaphase (panels a and a′), midcytokinesis (panels b and b′), late cytokinesis (panels c and c′), and interphase (panels d and d′). In panels a–d, staining of CYK-4 (green), microtubules (red), and DNA (blue) is shown. In panels a′–d′, staining of CYK-4 (green) and MKLP-1 (red) is shown. The scale bars indicate 10 μm.

(C) HeLa cells were depleted of HsCYK-4 using siRNAs and fixed, and CYK-4 (green), microtubules (red), and DNA (blue) were labeled. After 72 hr, anaphase figures were observed in which the central spindle was not well organized. Additionally, a significant fraction of cells in the culture became multinucleate or polyploid.

(D) HeLa cell lysates were analyzed by sucrose density gradient centrifugation followed by blotting with anti-MKLP-1 antibody or anti-HsCYK-4 antibody. HsCYK-4 and MKLP-1 cosediment at 8 S. The lowest band reacting with the CYK-4 antibody is caused by proteolysis of the N terminus.

(E) MKLP-1 and HsCYK-4 complex was immunoprecipitated from a microtubule binding fraction (MTfr.) of mitotic HeLa cells with specific antibodies. The 110 kDa and the faint 116 kDa bands were identified by mass spectrometry as MKLP-1. The 75 kDa band was identified by mass spectrometry as HsCYK-4. Broad bands at 50 kDa and near the gel front are derived from the immunoglobulin stripped from the affinity resin.

CYK-4 revealed that the bundles assembled with the centralspindlin complex were invariably associated with multiple foci of CYK-4 (Figure 6B, panels a–c). Likewise, the smaller bundles induced by ZEN-4 alone are associated with discrete foci of ZEN-4 (Figure 6B, panels d–f). Microtubule bundling was not observed when the full-length CYK-4 was substituted by a deletion mutant that lacks the N-terminal 34 residues and cannot bind to ZEN-4 (Figure 6C). We conclude that centralspindlin is sufficient to form large microtubule bundles in vitro and that this reaction depends on the presence of both constituents of the complex and their ability to physically interact.

We had noticed that the solubility of purified centralspindlin was salt sensitive. To systematically examine this behavior, the purified complex was diluted into buffers containing different amounts of salt and the preparation was centrifuged and the amount of protein remaining in the supernatant was compared to the amount initially present (Figure 6D). At 200 mM salt and

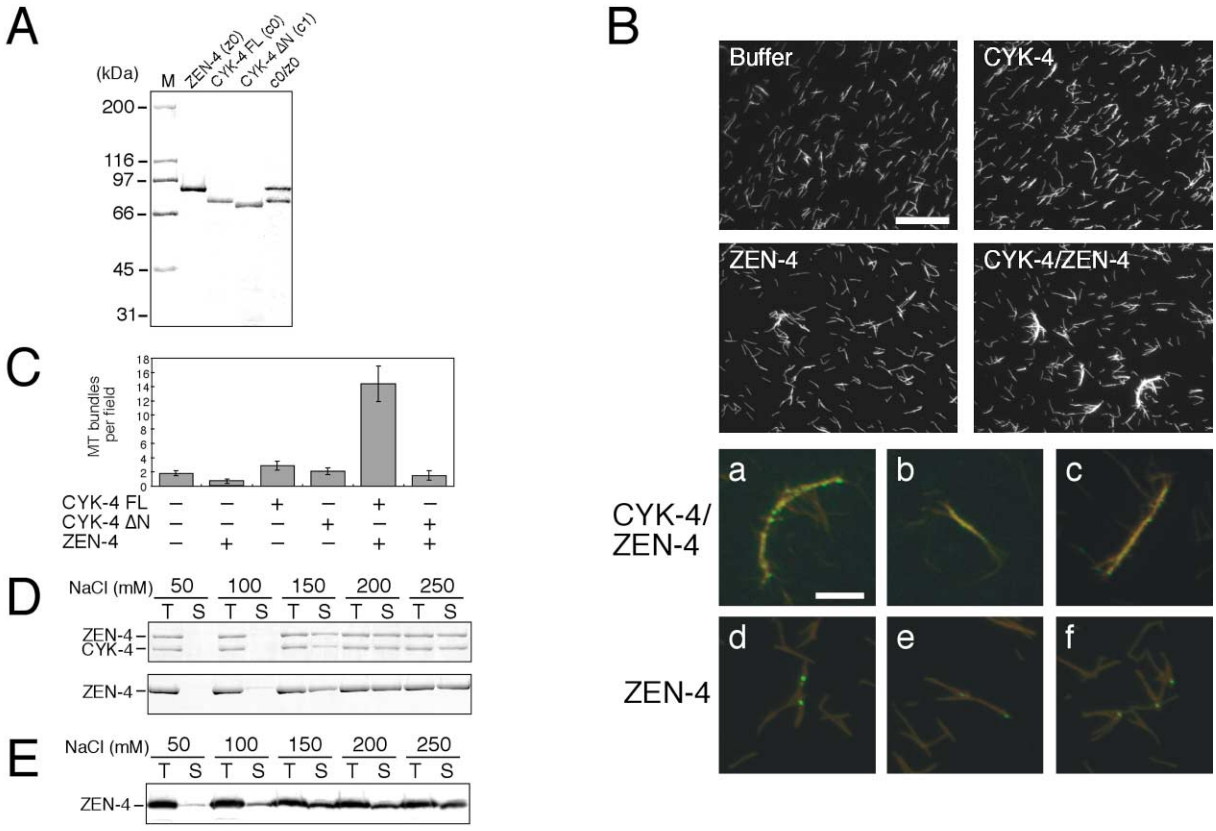

Figure 6. Recombinant Centralspindlin Promotes Microtubule Bundling In Vitro and Self-Associates into Higher Order Oligomers

(A) Preparation of recombinant CYK-4, ZEN-4, and the reconstituted centralspindlin complex. The purified protein preparations are shown.

(B) CYK-4 and/or ZEN-4 were incubated with taxol-stabilized microtubules, fixed, and sedimented onto glass coverslips. Tubulin and CYK-4 or ZEN-4 were stained with specific antibodies. The upper panels show the distribution of microtubules (the scale bar indicates 20 μm); the lower panels show high magnification views of tubulin/CYK-4 (panels a–c) and tubulin/ZEN-4 (panels d–f; the scale bar indicates 5 μm).

(C) The extent of microtubule bundling induced by ZEN-4, CYK-4, or CYK-4 derivative (c1) lacking the N-terminal 34 residues alone or in combination was quantitated. Ten random fields of samples prepared as in (B) were imaged and the number of microtubules bundled per field (± SEM) were automatically counted; a microtubule bundle was defined as an object with an intensity >3.5 times that of a single microtubule.

(D) Centralspindlin and ZEN-4 exhibit salt-sensitive solubility. The solubility of centralspindlin and ZEN-4 alone were assayed after dilution into buffers with the indicated ionic strengths; shown is a Coomassie-stained gel.

(E) Centralspindlin solubility is also salt sensitive in *C. elegans* embryo extracts. *C. elegans* embryos were lysed under low salt conditions; NaCl was added to the indicated concentrations and the solubility was assayed as above by Western blotting with anti-ZEN-4 antibodies.

higher, the complex was entirely soluble. As the salt concentration was reduced, centralspindlin became less soluble. The ZEN-4 subunit alone behaved essentially the same, suggesting that this behavior was governed by this constituent of the complex. When crude extracts from *C. elegans* embryos were used as a source of centralspindlin, similar results were obtained (Figure 6E). These data suggest that centralspindlin forms higher order structures. Such structures might contribute to its ability to bundle microtubules.

Discussion

Recent studies indicate that the central spindle is a structure that is essential for completion of cytokinesis. Two proteins required for central spindle assembly, CYK-4 and ZEN-4, were previously known to colocalize to the central spindle and to act in concert with one another, but the mechanism was entirely unclear. In this study, we have demonstrated that in vivo, CYK-4 and ZEN-4 are present in an evolutionarily conserved protein complex and we have characterized in detail the nature of this complex in *C. elegans* embryos and in human cells. These data suggest that the CYK-4/ZEN-4 complex, which we have named centralspindlin, consists of two molecules each of CYK-4 and ZEN-4. CYK-4 binds to the neck region of the ZEN-4 kinesin, raising the possibility that the motor activity of ZEN-4 is directly regulated by CYK-4. Moreover, the combination of CYK-4 and ZEN-4 is sufficient to bundle microtubules in vitro.

Architecture of the Centralspindlin Complex

Analytical biochemistry of the native centralspindlin complex isolated from *C. elegans* embryos demonstrates the existence of a complex containing the ZEN-4 kinesin and the CYK-4 RhoGAP. We have used in vitro binding experiments to define the critical determinants of this

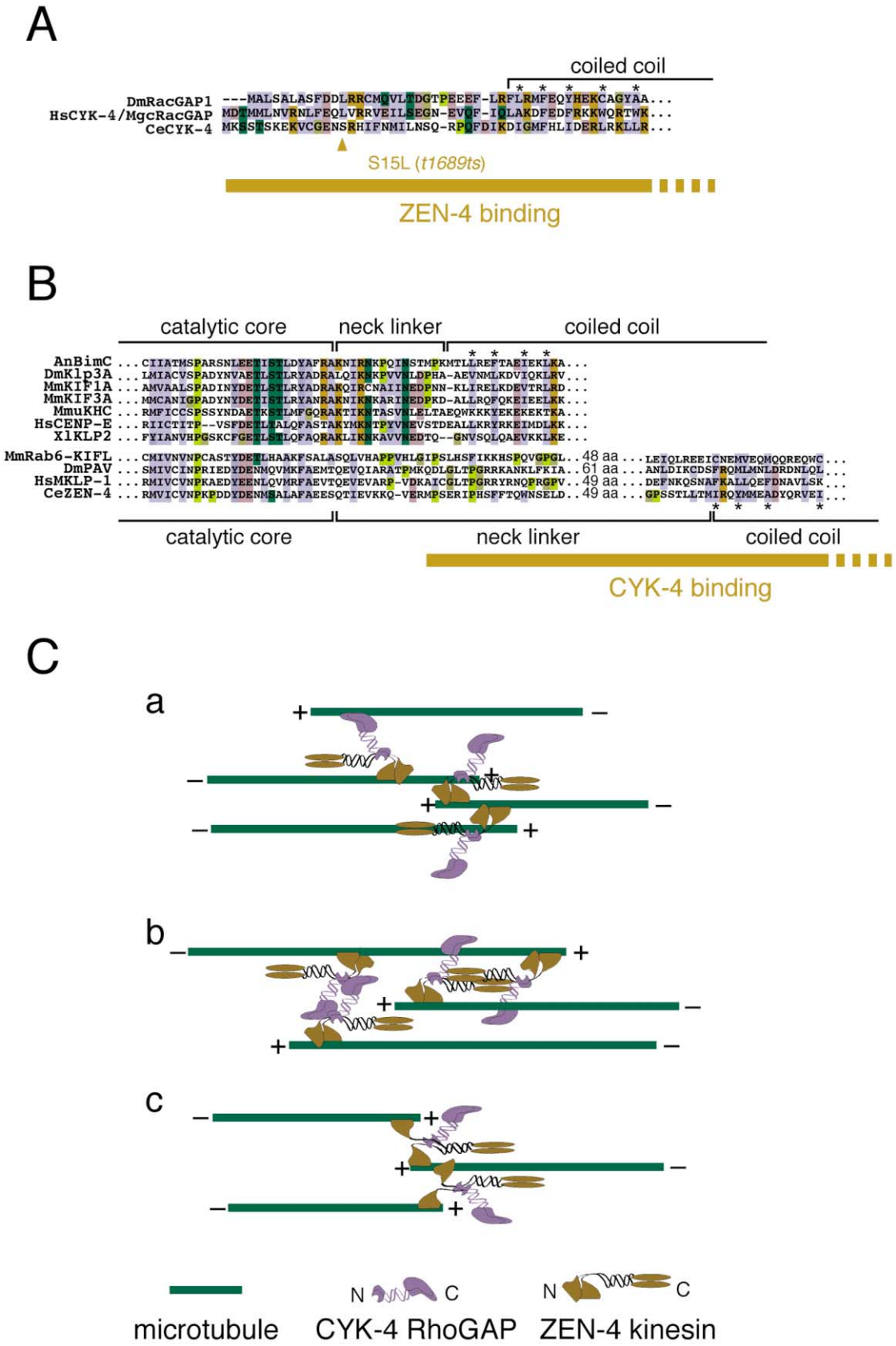

Figure 7. Centralspindlin and Its Role in the Formation of the Central Spindle

(A) Sequence comparison of the N-terminal region of CYK-4. This domain, though functionally important, is not well conserved.

(B) Sequence comparison of the neck linker region of various N kinesins to the MKLP-1 subfamily. Note that a number of highly conserved residues in the neck linker region are not conserved in the MKLP-1 subfamily.

(C) A schematic view of the centralspindlin complex and three possible models for how it might mediate central spindle assembly. See text for details.

interaction and to demonstrate that the two subunits are able to individually self-associate. Genetic and biochemical suppression of CYK-4(S15L) by mutations in ZEN-4 strongly argues that the interaction between CYK-4 and ZEN-4 is critical for CYK-4 function. Indeed, in vivo, the majority of ZEN-4 is in a complex with CYK-4. Surprisingly, the primary structure of the N-terminal region of CYK-4 is not well conserved (Figure 7A). However, the function is likely conserved, since the N-terminal 120 residues of HsCYK-4 are sufficient to localize in cultured mammalian cells (data not shown). In addition, the ortholog of CYK-4 is required for cytokinesis in mammalian cells (this study) and in mouse embryos (Van de Putte et al., 2001). Moreover, five pieces of evidence together indicate that HsCYK-4 and MKLP-1 are in a tetrameric complex. First, immunopurification of HsCYK-4 and MKLP-1 recovered equimolar amounts of the two proteins. Second, these two proteins comigrate on sucrose density gradients with a similar S value as observed for the *C. elegans* proteins. Third, the two proteins comigrate on a gel filtration column and their fractionation behavior suggests a native molecular mass for the complex of ~300 kDa. Fourth, upon reconstitution of the complex in insect cells, equimolar amounts of CYK-4 copurified with ZEN-4. Fifth, both CYK-4 and ZEN-4 are able to individually multimerize. Previous determinations of the native molecular mass of MKLP-1 have been reported, and the values are similar to those we present here (Chui et al., 2000; Kuriyama et al., 1994). These studies had not taken the presence of CYK-4 into consideration, and therefore the data was interpreted to indicate that MKLP-1 exists as a homotetramer. In contrast, our results indicate that the centralspindlin complex is a tetramer containing two molecules of the ZEN-4/MKLP-1 kinesin and two molecules of the CYK-4 RhoGAP (Figure 7B).

Potential Regulation of the Motor Domain by CYK-4

CYK-4 binds to ZEN-4 in a particularly interesting domain of this kinesin family member. A critical element of the kinesin molecule lies just C-terminal to the catalytic core—the neck linker region. ATP binding to one catalytic core induces a large conformational change in the neck linker region that causes the other catalytic core present in the kinesin dimer to extend toward the adjacent tubulin subunit situated on the plus side of the initial microtubule contact (Kikkawa et al., 2001; Rice et al., 1999). CYK-4 binds to a region of ZEN-4 that includes the neck linker region. In conventional kinesin, the neck linker corresponds to a region 15 amino acids long that connects the catalytic core of kinesin to the coiled-coil stalk domain. Among the family of KIN-N motors, the MKLP-1 subfamily has a distinctly divergent neck linker region; it lacks several nearly invariant residues, and the linker between the catalytic core and the coiled-coil region is about five times longer than in other members of the KIN-N family (Figure 7B). The divergence of this critical region of the kinesin suggests that MKLP-1-mediated microtubule motility may differ from that of other kinesins. Moreover, since CYK-4 binds to the neck linker region of ZEN-4, it is possible that CYK-4 binding may in fact regulate ZEN-4 motor activity.

Mode of Microtubule Crosslinking

The centralspindlin complex we have characterized appears to contain two kinesin motors and two RhoGAP molecules. Since most kinesin motors are dimers in which both catalytic cores interact with a single microtubule protofilament, the subunit composition we have described for the complex does not easily explain how microtubule bundling is achieved. If the two kinesin subunits of centralspindlin bind to the same microtubule protofilament, how might microtubule crosslinking occur? At this point, we can envisage at least three possible, though not mutually exclusive, mechanisms (Figure 7B).

The first possibility is that there is an additional microtubule binding site elsewhere in the CYK-4/ZEN-4 complex. No additional binding site has been identified yet in CYK-4, nor has MKLP-1, ZEN-4, or Pav been found to have an additional microtubule binding site. However, it has been shown, and we have confirmed (data not shown), that MKLP-1 interacts differently with microtubules than most kinesin-like proteins. Specifically, ATP is usually sufficient to elute most kinesins from microtubules, but in the case of MKLP-1, both ATP and high salt are required (Kuriyama et al., 1994; Nislow et al., 1992). Thus it is possible that MKLP-1 interacts with two microtubules, one by the motor domain and another via a different interaction surface. Consistent with this possibility is the finding that Rab6KIFL kinesin, which is quite similar to MKLP-1 in primary structure as well as in its localization and proposed function (Fontijn et al., 2001; Hill et al., 2000), contains a second microtubule binding activity in the C-terminal half of the molecule (Echard et al., 1998). However, this possibility does not explain why CYK-4 is required for central spindle assembly.

The second alternative is that MKLP-1 forms higher order structures and that the tetramer that we have characterized is a building block. This possibility gains some support from the biochemical characterization of centralspindlin. In vitro, centralspindlin forms higher order complexes at physiological ionic strength. Further support of this possibility comes from localization studies; in both *C. elegans* and mammalian cells, we find ring-like structures that we term division remnants that persist in the cell cortex after division. These remnants appear to be large aggregates of centralspindlin which are not in obvious association with microtubule bundles. Higher order oligomers could potentially form in early anaphase and promote microtubule bundling. This model is conceptually similar to the mechanism by which myosin II filaments promote the formation of antiparallel bundles of actin filaments.

The third possibility is that, unlike most N-terminal kinesins, the two catalytic cores of the kinesin subunits in the centralspindlin complex could bind to different microtubules. This would not be without precedent, in that the KIN-N KIF1A moves processively along a microtubule using a single head (Okada and Hirokawa, 2000). The association of the two catalytic cores of MKLP-1 with different microtubules is made feasible by the fact that the linker region between the catalytic core and the coiled-coil domain is much longer than that present in most N-terminal kinesins (Figure 7B). Perhaps CYK-4 ensures that the two motor domains are oriented in such

a way to bind to antiparallel microtubules (Figure 7C). Structural analysis of centralspindlin will help to define the mechanism of antiparallel microtubule bundling.

Several lines of evidence suggest that centralspindlin may be regulated by at least two different kinases. Genetic analysis indicates that Pav localization requires Polo kinase (Carmena et al., 1998). In addition, the Aurora-B/Incenp complex is also required for the stable localization of centralspindlin in *C. elegans* embryos (Kaitna et al., 2000), and an in vitro biochemical interaction has been detected between Aurora-B (AIR-2) and ZEN-4 (Severson et al., 2000). Reconstitution of central spindle assembly in vitro will allow the role of these and other regulators of centralspindlin to be dissected.

Experimental Procedures

Worm Strains and Alleles

The following strains or alleles were used in this study: N2 (Bristol), CB4856, *cyk-4(t1689ts)*, *unc-64*, *bli-6(sc16)*, *unc-24(e138)*, *unc-44(e1260)*, *lag-1(q385)*, and *mIs11 IV*. Some strains were obtained from the *C. elegans* Genetics Center (CGC). The CGC is funded by the National Center for Research Resources of the National Institutes of Health (NIH).

Isolation of *cyk-4* Suppressors

Suppressors of the *cyk-4(t1689ts)* mutation were obtained by mutagenizing *cyk-4(t1689ts)* animals with 30–40 mM EMS or 0.5 mM ENU. After recovery, the F1 embryos were isolated by bleaching and then allowed to grow at the permissive temperature. When F2 animals reached early adulthood, the population was shifted to 20°C and fertile animals were selected. Approximately 100,000 F1 genomes were screened and 18 suppressor mutations, all but two being unambiguously independent, were isolated. All of the suppressor strains were viable and fertile at 20°C, but none were able to grow at 25°C. Six intragenic suppressor mutations were identified. The ZEN-4 coding region of the remaining mutants was sequenced and seven strains were found to contain substitutions in the *zen-4* locus (Figure 3A). Of the remaining five suppressors, four were weak; none have been characterized in any detail. To confirm that the substitution in *zen-4(xs82)* was responsible for the suppressing activity, suppressor activity was mapped to less than 1 cM surrounding the *zen-4* locus.

RNA Interference

RNA interference was performed using siRNAs (Dharmacon Research; 5′-CCUCUUCUGACCUUUCGCCdTdT-3′ and 5′-GGCGAAA GGUCAGAAGAGGdTdT-3′) as described (Elbashir et al., 2001).

Antibodies

Rabbit CYK-4-specific and ZEN-4-specific antisera were reported previously (Jantsch-Plunger et al., 2000). CYK-4 and ZEN-4 antibodies were affinity purified with His6-CYK-4 (407–613) or His6-ZEN-4 (578–775) immobilized on NHS-Sepharose (Pharmacia).

MKLP-1-specific antisera and HsCYK-4-specific antisera were produced in rabbits and mice (Gramsch Laboratories, Schwabhausen, Germany) using C-terminal peptides (QLGPGYQHHAQPKR KKP and SKSKSATNLGRQGNFFASPMLK, respectively) conjugated to keyhole limpet hemocyanin as immunogens. Rabbit antibodies were affinity purified using peptides immobilized on Poros epoxide resin.

In Vitro Binding Assays

CYK-4, ZEN-4, and fragments thereof were expressed by in vitro transcription and translation systems with reticulocyte lysates using the TNT-coupled reticulocyte lysate system (Promega) or the PROTEINscript™ II (Ambion) kits, typically in 20 μl reactions. Full-length proteins without tags were expressed from the T3 promoter of pBluescript SK(−). Fragments of CYK-4 and ZEN-4 tagged with chitin binding domain (CBD) at the N terminus were expressed from the T7 promoter of pCBD-TEV. Following translation, the products were diluted in 100 μl buffer A and incubated at 20°C for 30 min (buffer A: 20 mM HEPES, 150 mM NaCl, 2 mM $MgCl_2$, 10 mM EDTA, 1 mM DTT, 1 mM PMSF, 10 μg/ml leupeptin, 10 μg/ml pepstatin, 10 μg/ml chymostatin) with 0.5% (w/v) Triton X-100. ZEN-4 or CYK-4 proteins were immunoprecipitated with specific antibodies or affinity purified by chitin beads. For immunoprecipitation, 0.5 μg antibody was added to the reactions and incubated on ice for 1 hr, followed by incubation with 5 μl protein A-Sepharose beads at 4°C for 1 hr. For CBD affinity purification, 5 μl of chitin beads (New England Biolabs) was added. In both cases, the beads were washed three times with buffer A containing 0.5% (w/v) Triton X-100. Proteins bound to the beads were analyzed by SDS-PAGE followed by autoradiography with a phosphoimager.

Preparation of Cell Lysates

C. elegans embryos were prepared by bleaching a synchronous culture of adult worms grown on "egg plates" as described (Lewis and Fleming, 1995). Embryos were washed with buffer A without Triton X-100 and frozen in liquid nitrogen and stored at −80°C. Embryos were crushed by grinding them in a mortar and pestle in liquid nitrogen. Cellular debris was removed by brief centrifugation.

HeLa cells were synchronized by treatment with 0.1 μg/ml nocodazole for 16 hr. Cells were washed twice with cold PBS, frozen in liquid nitrogen, and stored at −80°C. Cells were lysed and thawed by resuspension into ten volumes of buffer A with 0.5% (w/v) Triton X-100.

Preparation of Microtubule Binding Fraction

A frozen pellet (0.5 ml) of nocodazole-arrested cells was thawed and lysed in 5 ml of ice-cold BRB80 (80 mM K PIPES, 1 mM $MgCl_2$, 1 mM EGTA [pH 6.8]) with 0.1% (w/v) Triton X-100. The lysate was clarified by centrifugation at 10,000 × g for 15 min. The resulting supernatant was centrifuged at 25,000 × g for 20 min at 4°C in a S100AT6 rotor (Hitachi). Microtubules polymerized with glycerol and taxol were added to the supernatant. After incubating at 20°C for 20 min, microtubules were pelleted by centrifugation at 25,000 × g for 20 min at 20°C. The bound proteins were released from microtubules by incubation in 0.5 M NaCl, 5 mM ATP in BRB80 at 20°C for 20 min, followed by centrifugation at 25,000 × g for 20 min at 20°C.

Mass Spectrometry Analysis

Peptides were excised from SDS-PAGE gels, digested with trypsin, and extracted with 50 mM ammonium bicarbonate and then with 5% formic acid. Extracted supernatants were collected and injected into a NanoHPLC (LC Packings) coupled to an LCQ ion trap mass spectrometer (Finnigan). Collected MS/MS spectra were searched against a nonredundant database using MASCOT software. Each sample matched more than 20 peptides of the indicated proteins.

Hydrodynamics

Sedimentation coefficients were estimated by ultracentrifugation through a 2 ml linear gradient of 5%–20% (w/v) sucrose in buffer A (+ 0.6 M NaCl) without Triton X-100 using an S55S rotor (Hitachi). A 150 μl cell lysate or microtubule binding fraction was applied. Chicken ovalbumin (3.4 S), bovine γ-globulin (7.1 S), bovine catalase (11 S), and bovine thyroglobulin (19 S) were used as standards. The diffusion coefficient was estimated by gel filtration using a Superdex 200 column (30 ml) on an FPLC system (Pharmacia).

Immunoprecipitation and Western Blotting

Lysates (500 μl) were precleared with 50 μl protein A-Sepharose beads. For immunoprecipitation from worm embryos, 1 μg of affinity-purified antibody was added to the lysate. After incubation on ice for 1 hr, the immunocomplex was recovered by incubation with 5 μl protein A-Sepharose (Pharmacia) at 4°C for 1 hr. For immunoprecipitation from HeLa cells, antibodies were covalently immobilized on protein A beads (1 μg per 1 μl beads) with dimethyl pimelimidate. The precleared lysate was incubated with antibody beads at 4°C for 1–4 hr. The beads were washed three times with buffer A plus 0.5% Triton X-100.

For Western blotting, samples were run on a 7.5% SDS-PAGE gel and electrotransferred to a nitrocellulose membrane (HiBond ECL; Amersham).

Baculovirus Expression

Recombinant baculoviruses were produced in Sf9 cells using the Bac-to-Bac system according to the manufacturer's instructions. Recombinant proteins were expressed in High-Five cells. Cells were harvested at 60 hr after viral infection. After washing once with PBS, cells were lysed with 250 mM NaCl, 0.1% Triton X-100, 20 mM HEPES-NaOH, 1 mM EGTA, 1 mM $MgCl_2$, 0.1 mM ATP, 1 mM DTT, 10 μg/ml leupeptin, 10 μg/ml pepstatin, 1 mM PMSF (pH 7.7). For CYK-4 His6, DTT was replaced with 5 mM β-mercaptoethanol. Following centrifugation at 20,000 $\times$ g for 20 min, the supernatants were applied to chitin beads or Ni-NTA resin. After washing, ZEN-4 was eluted by cleavage of the linker with TEV protease. CYK-4 was eluted by a stepwise increase of imidazole from 20 mM to 100 mM. Recombinant centralspindlin was produced by coinfection with CYK-4- and ZEN-4-expressing viruses and purification using the CBD tag fused to ZEN-4. The TEV protease was used for elution.

Microtubule Bundling Assay

To reconstitute the CYK-4/ZEN-4 complex, equimolar ($\sim$1 μM) amounts of recombinant CYK-4 and ZEN-4 were mixed and incubated for 15 min at room temperature. Samples (final 0.1 μM) were mixed with taxol-stabilized microtubules (final 4 μM) in 150 mM KCl, 80 mM PIPES, 1 mM EGTA, 1 mM $MgCl_2$, 1 mM DTT, 5 mM AMP-PNP (pH 6.8) and incubated for 15 min at room temperature. The reaction was fixed with glutaraldehyde and the microtubules were sedimented on a coverslip as described (Desai and Walczak, 2001). Microtubules and CYK-4/ZEN-4 were stained with anti-tubulin monoclonal antibody (DM1α) and either anti-CYK-4 or anti-ZEN-4 rabbit polyclonal antibody.

Centralspindlin Sedimentation Assay

Samples (final 20 μg/ml) were diluted in 20 mM HEPES, 1 mM EGTA, 1 mM $MgCl_2$, 0.1 mM ATP, 1 mM DTT, and the indicated final concentration of NaCl. Following incubation for 30 min at 25°C, a portion of the reaction was removed (total) and the remainder was centrifuged at 10,000 $\times$ g for 30 min at 25°C. The total and supernatant fractions were analyzed by SDS-PAGE and Coomassie staining or Western blotting.

Immunolocalization

Immunolocalization studies using HeLa cells were performed according to standard procedures following fixation in $-$20°C methanol.

Acknowledgments

We thank Karl Mechtler for exceptional mass spectrometry analysis. We also thank Gerard Gacon (INSERM) for the kind gift of antibodies to HsCYK-4/MgcRacGAP that were used in the initial stages of this study. We thank Steven Wicks and Ronald Plasterk for sharing unpublished SNP data. We thank Reinhard Dechant, Juergen Knoblich, Manuel Mendoza, Alper Romano, and Jan-Michael Peters for comments that improved the manuscript. This work was supported by Boehringer Ingelheim.

Received April 23, 2001; revised November 26, 2001.

References

Adams, R.R., Tavares, A.A., Salzberg, A., Bellen, H.J., and Glover, D.M. (1998). pavarotti encodes a kinesin-like protein required to organize the central spindle and contractile ring for cytokinesis. Genes Dev. *12*, 1483–1494.

Carmena, M., Riparbelli, M.G., Minestrini, G., Tavares, A.M., Adams, R., Callaini, G., and Glover, D.M. (1998). *Drosophila* polo kinase is required for cytokinesis. J. Cell Biol. *143*, 659–671.

Case, R.B., Rice, S., Hart, C.L., Ly, B., and Vale, R.D. (2000). Role of the kinesin neck linker and catalytic core in microtubule-based motility. Curr. Biol. *10*, 157–160.

Chui, K.K., Rogers, G.C., Kashina, A.M., Wedaman, K.P., Sharp, D.J., Nguyen, D.T., Wilt, F., and Scholey, J.M. (2000). Roles of two homotetrameric kinesins in sea urchin embryonic cell division. J. Biol. Chem. *275*, 38005–38011.

Desai, A., and Walczak, C.E. (2001). Assays for microtubule-destabilizing kinesins. Methods Mol. Biol. *164*, 109–121.

Echard, A., Jollivet, F., Martinez, O., Lacapere, J.J., Rousselet, A., Janoueix-Lerosey, I., and Goud, B. (1998). Interaction of a Golgi-associated kinesin-like protein with Rab6. Science *279*, 580–585.

Elbashir, S.M., Harborth, J., Lendeckel, W., Yalcin, A., Weber, K., and Tuschl, T. (2001). Duplexes of 21-nucleotide RNAs mediate RNA interference in cultured mammalian cells. Nature *411*, 494–498.

Fontijn, R.D., Goud, B., Echard, A., Jollivet, F., van Marle, J., Pannekoek, H., and Horrevoets, A.J. (2001). The human kinesin-like protein RB6K is under tight cell cycle control and is essential for cytokinesis. Mol. Cell. Biol. *21*, 2944–2955.

Hill, E., Clarke, M., and Barr, F.A. (2000). The Rab6-binding kinesin, Rab6-KIFL, is required for cytokinesis. EMBO J. *19*, 5711–5719.

Hirose, K., Kawashima, T., Iwamoto, I., Nosaka, T., and Kitamura, T. (2001). MgcRacGAP is involved in cytokinesis through associating with mitotic spindle and midbody. J. Biol. Chem. *276*, 5821–5828.

Hurley, J.H., and Meyer, T. (2001). Subcellular targeting by membrane lipids. Curr. Opin. Cell Biol. *13*, 146–152.

Jantsch-Plunger, V., Gönczy, P., Romano, A., Schnabel, H., Hamill, D., Schnabel, R., Hyman, A.A., and Glotzer, M. (2000). CYK-4. A rho family GTPase activating protein (gap) required for central spindle formation and cytokinesis. J. Cell Biol. *149*, 1391–1404.

Kaitna, S., Mendoza, M., Jantsch-Plunger, V., and Glotzer, M. (2000). Incenp and an aurora-like kinase form a complex essential for chromosome segregation and efficient completion of cytokinesis. Curr. Biol. *10*, 1172–1181.

Kikkawa, M., Sablin, E.P., Okada, Y., Yajima, H., Fletterick, R.J., and Hirokawa, N. (2001). Switch-based mechanism of kinesin motors. Nature *411*, 439–445.

Kull, F.J., Sablin, E.P., Lau, R., Fletterick, R.J., and Vale, R.D. (1996). Crystal structure of the kinesin motor domain reveals a structural similarity to myosin. Nature *380*, 550–555.

Kuriyama, R., Dragas-Granoic, S., Maekawa, T., Vassilev, A., Khodjakov, A., and Kobayashi, H. (1994). Heterogeneity and microtubule interaction of the CHO1 antigen, a mitosis-specific kinesin-like protein. Analysis of subdomains expressed in insect Sf9 cells. J. Cell Sci. *107*, 3485–3499.

Lewis, J.A., and Fleming, J.T. (1995). Basic culture methods. Methods Cell Biol. *48*, 3–29.

Mastronarde, D.N., McDonald, K.L., Ding, R., and McIntosh, J.R. (1993). Interpolar spindle microtubules in PTK cells. J. Cell Biol. *123*, 1475–1489.

Nislow, C., Lombillo, V.A., Kuriyama, R., and McIntosh, J.R. (1992). A plus-end-directed motor enzyme that moves antiparallel microtubules in vitro localizes to the interzone of mitotic spindles. Nature *359*, 543–547.

Okada, Y., and Hirokawa, N. (2000). Mechanism of the single-headed processivity: diffusional anchoring between the K-loop of kinesin and the C terminus of tubulin. Proc. Natl. Acad. Sci. USA *97*, 640–645.

Powers, J., Bossinger, O., Rose, D., Strome, S., and Saxton, W. (1998). A nematode kinesin required for cleavage furrow advancement. Curr. Biol. *8*, 1133–1136.

Raich, W.B., Moran, A.N., Rothman, J.H., and Hardin, J. (1998). Cytokinesis and midzone microtubule organization in *Caenorhabditis elegans* require the kinesin-like protein ZEN-4. Mol. Biol. Cell *9*, 2037–2049.

Rice, S., Lin, A.W., Safer, D., Hart, C.L., Naber, N., Carragher, B.O., Cain, S.M., Pechatnikova, E., Wilson-Kubalek, E.M., Whittaker, M., et al. (1999). A structural change in the kinesin motor protein that drives motility. Nature *402*, 778–784.

Sablin, E.P., Kull, F.J., Cooke, R., Vale, R.D., and Fletterick, R.J. (1996). Crystal structure of the motor domain of the kinesin-related motor ncd. Nature *380*, 555–559.

Saxton, W.M., and McIntosh, J.R. (1987). Interzone microtubule behavior in late anaphase and telophase spindles. J. Cell Biol. *105*, 875–886.

Sellitto, C., and Kuriyama, R. (1988). Distribution of a matrix component of the midbody during the cell cycle in Chinese hamster ovary cells. J. Cell Biol. *106*, 431–439.

Severson, A.F., Hamill, D.R., Carter, J.C., Schumacher, J., and Bowerman, B. (2000). The aurora-related kinase AIR-2 recruits ZEN-4/CeMKLP1 to the mitotic spindle at metaphase and is required for cytokinesis. Curr. Biol. *10*, 1162–1171.

Sharp, D.J., Kuriyama, R., and Baas, P.W. (1996). Expression of a kinesin-related motor protein induces Sf9 cells to form dendrite-like processes with nonuniform microtubule polarity orientation. J. Neurosci. *16*, 4370–4375.

Straight, A.F., and Field, C.M. (2000). Microtubules, membranes and cytokinesis. Curr. Biol. *10*, R760–R770.

Toure, A., Dorseuil, O., Morin, L., Timmons, P., Jegou, B., Reibel, L., and Gacon, G. (1998). MgcRacGAP, a new human GTPase-activating protein for Rac and Cdc42 similar to *Drosophila* rotundRacGAP gene product, is expressed in male germ cells. J. Biol. Chem. *273*, 6019–6023.

Vale, R.D., and Fletterick, R.J. (1997). The design plan of kinesin motors. Annu. Rev. Cell Dev. Biol. *13*, 745–777.

Vale, R.D., and Milligan, R.A. (2000). The way things move: looking under the hood of molecular motor proteins. Science *288*, 88–95.

Van de Putte, T., Zwijsen, A., Lonnoy, O., Rybin, V., Cozijnsen, M., Francis, A., Baekelandt, V., Kozak, C.A., Zerial, M., and Huylebroeck, D. (2001). Mice with a homozygous gene trap vector insertion in mgcRacGAP die during pre-implantation development. Mech. Dev. *102*, 33–44.

Wooltorton, E.J., Haliotis, T., and Mueller, C.R. (1999). Identification and characterization of a transcript for a novel Rac GTPase-activating protein in terminally differentiating 3T3-L1 adipocytes. DNA Cell Biol. *18*, 265–273.